

DNA Amplification and Hybridization Assays in Integrated Plastic Monolithic Devices

Yingjie Liu,* Cory B. Rauch, Randall L. Stevens, Ralf Lenigk, Jianing Yang, David B. Rhine, and Piotr Grodzinski*

Physical Sciences Research Laboratories, Motorola Labs, Motorola, Inc., 7700 South River Parkway, MD-ML34, Tempe, Arizona 85284

PCR amplification, DNA hybridization, and a hybridization wash have been integrated in a disposable monolithic DNA device, containing all of the necessary fluidic channels and reservoirs. These integrated devices were fabricated in polycarbonate plastic material by CO₂ laser machining and were assembled using a combination of thermal bonding and adhesive tape bonding. Pluronic polymer phase change valves were implemented in the devices to fulfill the valving requirements. Pluronic polymer material is PCR compatible, and 30% Pluronic polymer valves provide enough holding pressure to ensure a successful PCR amplification. By reducing the temperature locally, to ~5 °C, Pluronic valves were liquefied and easily opened. A hybridization channel was made functional by oligonucleotide deposition, using Motorola proprietary surface attachment chemistry. Reagent transport on the device was provided by syringe pumps, which were docked onto the device. Peltier thermal electrical devices powered the heating and cooling functionality of the device. Asymmetrical PCR amplification and subsequent hybridization detection of both *Escherichia coli* K-12 MG1655 and *Enterococcus faecalis* DNA genes have been successfully demonstrated in these disposable monolithic devices.

Genetic-based assays have a very wide range of applications in biotechnology and medicine, including agriculture, farming,¹ detection of pathogens in foods,² and genetic diagnostics on human subjects.^{3–5} The recent developments in molecular biology and genetic analysis have been outstanding. Technologies such as polymerase chain reaction (PCR) and DNA hybridization have become indispensable tools in the study of gene function, gene expression, and single-nucleotide polymorphisms (SNPs).^{6–10}

These powerful tools, for research and diagnostic applications, have triggered strong interests in the miniaturization of DNA analysis functions onto a single microfluidic chip.^{11,12}

The application of microfabrication technologies to the field of DNA diagnostics has created the potential to integrate biological sample preparation with DNA analysis in a single lab-on-a-chip device.^{11,12} The goal of this technology is to fully integrate multiple processes including sample collection, pretreatment with the DNA extraction, amplification, and detection on a single microfluidic platform. The ability to perform all of the steps of the biological assay, on a single self-contained microchip, promises significant advantages in terms of speed, cost, sample/reagent consumption, contamination reduction, efficiency, and automation.^{13–15}

The development of lab-on-a-chip technologies started with the miniaturization of conventional analytical tools. Capillary electrophoresis (CE) was among the earliest and most successful demonstrations of miniaturization.^{12,16,17} A variety of microstructures had also been proposed and constructed in order to perform PCR amplification in a microchip format. The majority of the existing micro-PCR devices are stand alone and constructed in silicon,^{18–21} glass,^{22–24} or fused-silica capillaries.²⁵ To generate temperatures necessary for an amplification reaction, most of these designs use resistive heaters surrounding the chambers while

- (1) Buitkamp, J.; Epplen, J. T. *Electrophoresis* **1996**, *17*, 1–11.
- (2) Feng, P. *Mol. Biotechnol.* **1997**, *7*, 267–278.
- (3) Collins, F. S. *Hosp. Pract.* **1991**, *26*, 93–98.
- (4) Cooper, D. N.; Schmidtko, J. *Hum. Genet.* **1993**, *92*, 211–236.
- (5) Mifflin, T. E. *J. Clin. Ligand Assay* **1996**, 27–42.
- (6) Duggan, D. J.; Bittner, M.; Chen, Y.; Meltzer, P.; Trent, J. M. *Nat. Genet.* **1999**, *21*, 10–14.
- (7) Lobenhofer, E. K.; Bushel, P. R.; Afshari, C. A.; Hamadeh, H. K. *Environ. Health Perspect.* **2001**, *109*, 881–891.
- (8) Noordewier, M. O.; Warren, P. V. *Trends Biotechnol.* **2001**, *19*, 412–415.
- (9) Maughan, N. J.; Lewis, F. A.; Smith, V. J. *Pathol.* **2001**, *195*, 3–6.
- (10) Dong, S.; Wang, E.; Hsie, L.; Cao, Y.; Chen, X.; Gingeras, T. R. *Genome Res.* **2001**, *11*, 1418–24.

- (11) Anderson, R. C.; Su, X.; Bogdan, G. J.; Fenton, J. *Nucleic Acids Res.* **2000**, *28*, E60.
- (12) Harrison, D. J.; Fluri, K.; Seiler, K.; Fan, Z.; Effenhauser, C. S.; Manz, A. *Science* **1993**, *261*, 895–897.
- (13) Wang, J. *Nucleic Acids Res.* **2000**, *28*, 3011–3016.
- (14) Ramsey, J. M.; Jacobson, S. C.; Knapp, M. R. *Nat. Med.* **1995**, *1*, 1093–1096.
- (15) Kricka, L. *Clin. Chim. Acta* **2001**, *307*, 219–223.
- (16) Manz, A.; Harrison, D. J.; Verpoorte, E.; Fetting, J. C.; Paulus, A.; Ludi, H.; Widmer, H. M. *J. Chromatogr.* **1992**, *593*, 253–258.
- (17) Jacobson, S. C.; Hergenroder, R.; Koutny, L. B.; Warmack, R. J.; Ramsey, J. M. *Anal. Chem.* **1994**, *66*, 1107–1113.
- (18) Wilding, P.; Shoffner, M. A.; Kricka, L. J. *Clin. Chem.* **1994**, *40*, 1815–1818.
- (19) Northrup, M. A.; Benett, B.; Hadley, D.; Landre, P.; Lehew, S.; Richards, J.; Stratton, P. *Anal. Chem.* **1998**, *70*, 918–922.
- (20) Chaudhari, A. M.; Woudenberg, T. M.; Albin, M.; Goodson, K. E. J. *Microelectromech. Syst.* **1998**, *7*, 345–355.
- (21) Daniel, J. H.; Iqbal, S.; Millington, R. B.; Moore, D. F.; Lowe, C. R.; Leslie, D. L.; Lee, M. A.; Pearce, M. J. *Sens. Actuators, A* **1998**, *81*, 81–88.
- (22) Oda, R. P.; Strausbauch, M. A.; Huhmer, A. F. R.; Borson, N.; Jurens, S. R.; Craighead, J.; Wettstein, P. J.; Eckloff, B.; Kline, B.; Landers, J. P. *Anal. Chem.* **1998**, *70*, 4361–4368.
- (23) Taylor, T. B.; Harvey, S. E.; Albin, M.; Lebak, L.; Ning, Y.; Mowat, I.; Schuerlein, T.; Principe, E. *Biomed. Microdevices* **1998**, *1*, 65–70.
- (24) Kopp, M.; De Mello, A.; Manz, A. *Science* **1998**, *280*, 1046–1048.
- (25) Zhang, N. Y.; Tan, H. D.; Yeung, E. S. *Anal. Chem.* **1999**, *71*, 1138–1145.

other designs utilize noncontact heating methods.²² As an alternative to static thermal cycling, device designs have used continuous flow through three heated regions^{24,26} to achieve rapid thermal cycling. Rapid thermal cycling as fast as 17 s/cycle has been demonstrated.²⁷

In recent years, progress in developing lab-on-a-chip technologies has occurred rapidly. Previously, an integrated microdevice demonstrated functions such as reagent mixing, enzymatic reaction, and DNA sizing by electrophoresis.²⁸ The integration of micro-PCR with microchip CE has also been developed and demonstrated in several laboratories.^{29–33} The devices reported by Burns et al.³⁴ are capable of metering aqueous reagents, mixing, amplifying, enzymatic digesting, electrophoretic separation, and detection with no external lenses, heaters, or mechanical pumps. Other integrated devices, demonstrated by Sosnowski et al.,³⁵ utilize electrical forces to accomplish such functions as cell separation, sample transport, hybridization acceleration, and denaturation. In another report,¹¹ integrated monolithic genetic assay devices have been fabricated in polycarbonate (PC) to carry out serial and parallel multistep molecular operations, including nucleic acid hybridization. In this work, the devices were fabricated by mechanical machining and assembled with screws and clamping fixtures. Recently, devices carrying out automated sample preparation followed by real-time PCR detection of pathogen have also been reported.³⁶

The overall performance of an integrated device depends not only on that of its individual functional units but also on that of the functional integration. As a result, microvalves have become the critical components for the further development of lab-on-a-chip technology. Some very ingenious microvalves have been designed and built as alternatives to silicon-based microvalves.^{37,38} Electrokinetic valves have been successfully used for sample injection in microchip CE, on-chip fluid mixing, and dilution.^{12,39} Hydrophobic passive valves have been implemented in microfabricated centrifugal microfluidic systems.⁴⁰ Systems containing on-off valves and switching valves have been built in elastomeric

materials by soft lithography.⁴¹ Polymer monoliths containing grafted thermally responsive polymer have been controlled thermally to block or allow flow in micrometer-size structures.⁴² Various designs of hydrogel valves, which operate on the principle of hydrogel volume change with external stimuli, have enabled the fabrication of an organic microfluidic system.⁴³ Because of the unique valving requirements (high pressure, biocompatibility, and device complexity) for the integration of PCR and hybridization functionality, none of these valves could be implemented into our monolithic integrated devices.

In this research, simple, low-cost, and disposable genetic assay devices were fabricated. PCR amplification, hybridization, and hybridization wash assays were demonstrated in monolithic integrated devices containing microfluidic channels. These microfluidic channels were fabricated into polycarbonate plastic by CO₂ laser machining. Reagent transport through the device was provided by syringe pumps, which were docked onto the device. Peltier thermal electrical devices powered the heating and cooling functionality of the device. Oligo probes were deposited inside the plastic hybridization channel using Motorola proprietary surface attachment chemistry, and the quality of probe attachment and dispensing was evaluated. Novel Pluronic phase change valves accomplished the integration of such functional units as PCR amplification, hybridization, and hybridization wash on the same device. An air-permeable hydrophobic membrane valve was implemented into the device to allow for the flow of solution into the sealed hybridization chamber. All of the reagents needed for the assay were loaded into the device before the assay. Genomic DNA from the bacteria *Escherichia coli* K-12 and *Enterococcus faecalis* were used to amplify *E. coli* K-12 MG1655 gene (221 bp) and *E. faecalis* DNAE gene (195 bp) by single or multiplex asymmetrical PCR (A-PCR). The single-strand amplicons were hybridized to the detection probes inside the hybridization channel. The performance of each individual functional unit and that of the integrated system is presented.

EXPERIMENTAL SECTION

Device Fabrication. To build low-cost, disposable microdevices, processes other than standard photolithography of silicon or glass are desired. Plastic materials are promising alternatives for building complex microelectromechanical systems and are easily machined by using many available techniques.^{33,44–47} Recently, UV laser photoablation has been used to fabricate microfluidic CE channel networks,⁴⁸ and infrared CO₂ laser has been used to create microchannels in PMMA.⁴⁹ In this work, we also explored the use of a CO₂ laser engraving system (Universal

- (26) Chiou, J.; Matsudaira, P.; Sonin, A.; Ehrlich, D. *Anal. Chem.* **2001**, *73*, 2018–2021.
- (27) Giordano, B. C.; Ferrance, J.; Swedberg, S.; Huhmer, A. F.; Landers, J. P. *Anal. Biochem.* **2001**, *291*, 124–132.
- (28) Jacobson, S. C.; Hergenroder, R.; Moore, A. W., Jr.; Ramsey, J. M. *Anal. Chem.* **1994**, *66*, 4127–4132.
- (29) Woolley, A. T.; Hadley, D.; Landre, P.; deMello, A. J.; Mathies, R. A.; Northrup, M. A. *Anal. Chem.* **1996**, *68*, 4081–4086.
- (30) Waters, L. C.; Jacobson, S. C.; Kroutchinina, N.; Khandurina, J.; Foote, R. S.; Ramsey, J. M. *Anal. Chem.* **1998**, *70*, 158–162.
- (31) Khandurina, J.; Meknight, T. E.; Jacobson, S. C.; Waters, L. C.; Foote, R. S.; Ramsey, J. M. *Anal. Chem.* **2000**, *72*, 2995–3000.
- (32) Lagally, E. T.; Medintz, I.; Mathies, R. A. *Anal. Chem.* **2001**, *73*, 565–570.
- (33) Liu, Y.; Ganser, D.; Schneider, A.; Liu, R.; Grodzinski, P.; Kroutchinina, N. *Anal. Chem.* **2001**, *73*, 4196–4201.
- (34) Burns, M. A.; Johnson, B. N.; Brahmasandra, S. N.; Handique, K.; Webster, J. R.; Krishnan, M.; Sammarco, T. S.; Man, P. M.; Jones, D.; Heldsinger, D.; Mastrangelo, C. H.; Burke, D. T. *Science* **1998**, *282*, 484–7.
- (35) Sosnowski, R. G.; Tu, E.; Butler, W. F.; O'Connell, J. P.; Heller, M. J. *Proc. Natl. Acad. Sci. U.S.A.* **1997**, *94*, 1119–1123.
- (36) Taylor, M. T.; Belgrader, P.; Joshi, R.; Kintz, G. A.; Northrup, M. A. In *Micro Total Analysis Systems 2001*; Ramsey, J. M., Van den Berg, A., Eds.; Kluwer Academic Publishers: New York, 2001; pp 670–672.
- (37) Smith, L.; Hok, B. *Proceedings of Transducers '91*, San Francisco, CA, 1991; pp 1049–1051.
- (38) Barth, P. W. *Proceedings of Transducers '95*, Stockholm, Sweden, 1995; pp 276–277.
- (39) Jacobson, S. C.; McKnight, T. E.; Ramsey, J. M. *Anal. Chem.* **1999**, *71*, 4455–4459.

- (40) Duffy, D. C.; Gillis, H. L.; Lin, J.; Sheppard, N. F.; Kellogg, G. L. *Anal. Chem.* **1999**, *71*, 4669–4678.
- (41) Unger, M. A.; Chou, H. P.; Thorsen, T.; Scherer, A.; Quake, S. R. *Science* **2000**, *288*, 113–116.
- (42) Peters, E. C.; Svec, F.; Frechet, J. M. J. *Adv. Mater.* **1999**, *11*, 1169–1181.
- (43) Beebe, D. J.; Moore, J. S.; Bauer, J. M.; Yu, Q.; Liu, R. H.; Devadoss, C.; Jo, B. H. *Nature* **2000**, *404*, 588–590.
- (44) Boerner, M.; Kohl, M.; Pantenburg, F.; Bacher, W.; Hein, H.; Schomburg, W. *Microsyst. Technol.* **1996**, *2*, 149–152.
- (45) Martynova, L.; Locascio, L. E.; Gaitan, M.; Kramer, G. W.; Christensen, R. G.; MacCrehan, W. A. *Anal. Chem.* **1997**, *69*, 4783–4789.
- (46) Xu, J.; Locascio, L.; Gaitan, M.; Lee, C. S. *Anal. Chem.* **2000**, *72*, 1930–1933.
- (47) Becker, H.; Dietz, W. *Proc. SPIE* **1998**, *3515*, 177–182.
- (48) Roberts, M. A.; Rossier, J. S.; Bercier, P.; Girault, H. *Anal. Chem.* **1997**, *69*, 2035–2042.

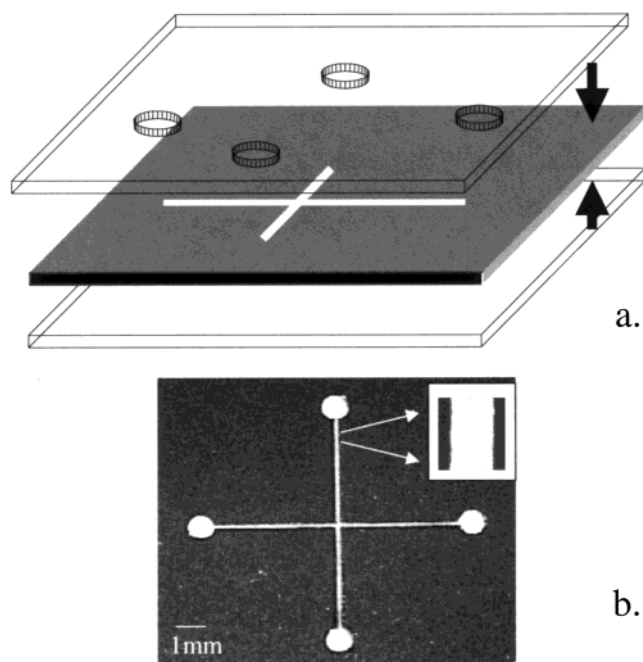


Figure 1. (a) Schematic of device fabrication process. The fluidic structure was fabricated on 250- μm black polycarbonate. The black polycarbonate was sandwiched between top and bottom transparent polycarbonate layers, and the assembly was thermally bonded. Access holes were fabricated on the top layer. (b) CO_2 laser-machined channel structure on a 250- μm thin black polycarbonate wafer. The width of the channel is 150 μm , and the holes at the end of the channels are 1 mm in diameter. A small portion of the channel was enlarged for better viewing.

Laser System Inc., Scottsdale, AZ) for device fabrication. Unlike UV photoablation, the CO_2 laser operates at a wavelength of 1060 nm with maximum output power of 40 W. When focused on the plastic work piece, the laser beam can either create channels in the work piece or cut completely through the work piece, depending on the laser power and writing speed. The device fabrication started with CO_2 laser cutting through a black PC wafer, which was 250 μm thick, to create the fluidic structure for PCR, valves, hybridization chamber, and various reservoirs. All of the CO_2 laser-machined fluidic devices were cleaned with isopropyl alcohol under a hood. The fluidic channel device was formed after the laser-machined black PC wafer was sandwiched between two transparent PC wafers of the same thickness and thermally bonded. A schematic of the fabrication procedure is shown in Figure 1a. Thermal bonding was carried out on Carver hydraulic laboratory presses (Carver, Inc. Wabash, IN) at 139 $^\circ\text{C}$ and under 2 tons of pressure for 45 min. The top transparent PC wafer contains all the fluidic access holes, which were also laser machined before bonding. The top PC wafer has a well-positioned square window of 1.7 cm long, such that, after bonding, the hybridization channel can be accessed through this window for surface treatment and oligo probe attachment. Following probe attachment, the hybridization channel was enclosed with a transparent PC piece of proper size using double-sided adhesive

tape. The hybridization channel portion of the device was pressed with 2 tons of pressure for 2 min to enforce the adhesive tape bonding. The edges of the square window were further sealed with 90-s epoxy.

PCR Amplification and Hybridization. The thermal cycler for micro-PCR was designed and built using two Peltier thermal electrical devices (1 in. \times 1 in., output power of 18.1 W). Aluminum blocks are attached to the backside of the Peltier devices as heat sinks, and a small cooling fan was also attached to each of the two aluminum blocks for convective cooling. During PCR thermal cycling, the serpentine PCR chamber portion of the device was sandwiched between the two Peltier elements by clamping the two aluminum blocks together. The device temperature and Peltier surface temperature were monitored using thermocouples, and LabView program was used for thermal cycle temperature control. The PCR protocol is 70 s at 94 $^\circ\text{C}$ for initial denaturation, followed by 36 cycles of 20 s each at 94, 55, and 72 $^\circ\text{C}$, respectively.

Asymmetrical PCR. Two genetic targets were asymmetrically amplified in the assays: *E. coli* K-12 MG1655 gene (221 bp) and *E. faecalis* DNAE gene (195 bp). The A-PCR reaction mixture contained 10 mM Tris-HCl (pH 8.3), 50 mM KCl, 1.5 mM MgCl_2 , 0.001% gelatin, 250 $\mu\text{g}/\text{mL}$ bovine serum albumin, 125 μM each deoxynucleotide triphosphate, 1.2 μM reverse primer, 12 nM forward primer, 25 units/mL AmpliTaq, DNA polymerase (Perkin-Elmer), and *E. faecalis* or *E. coli* genomic DNA (50 $\text{pg}/\mu\text{L}$). The primer set used to amplify a 221-bp segment of *E. coli* gene target is 5'-AAC GGC CAT CAA CAT CGA ATA CAT3' (forward) and 5'-[cy3] GGC GTT ATC CCC AGT TTT TAG TGA3' (reverse). The probe used for hybridization is AAG CGA CAG TTC GGC TTC GTG NH_2 3'. The primer set used to amplify *E. faecalis* gene is 5'-GCC AGA TTT TTC GTT CGC TCA T3' (forward) and 5'-[Cy3] AAA TCG GCA ACT TCT CGC TCA G (reverse). The probe used for hybridization is CGG AAG AAA GCT CTG AGC G NH_2 3'. The probe for negative control is AGC TCA CGT GCC TGC AGA AG NH_2 3'. All control PCR were performed on a DNA Engine Thermal Cycler from MJ Research Inc. (South San Francisco, CA). All the oligo probes and PCR primers were ordered from Operon Technology Inc. (Alameda, CA). PCR products were analyzed by Agilent 2100 bioanalyzer (Palo Alto, CA) using a DNA 500 assay on Caliper LabChips.

Oligonucleotide Immobilization and Hybridization. PC surfaces of the hybridization channels were activated using Motorola proprietary surface modification chemistry. UV protection glasses were needed during surface activation (model UVGL-58, UVP, Upland, CA). Amine-terminated oligonucleotide probes were prepared in 50 mM phosphate buffer, pH 8, with final oligo concentration of 20 μM . These probes were then immobilized onto a modified PC surface through end-point attachment. Oligo probes were spotted onto the activated PC microfluidic channels by using SpotBot Personal Microarrayer (TeleChem International, Inc., Sunnyvale, CA). The spotted chips were put in a humidity chamber (saturated NaCl water solution) for oligo attachment reaction overnight. The chips were then washed with TNTw buffer (10 mM Tris-HCl, pH 7.5, 150 mM NaCl, 0.05% Tween-20) and then water to remove any unattached oligos. The quality of probe attachment and probe dispensing was evaluated using standalone hybridization channel devices. The probes used for this study are 5'-Cy3T₁₀NH₂, and D3488 (5'-cy3 AAG CGA CAG TTC GGC TTC

(49) Goranovic, G.; Klank, H.; Westergaard, C.; Geschke, O.; Telleman, P.; Kutter, J. P. In *Micro Total Analysis Systems 2001*; Ramsey, J. M., Van den Berg, A., Eds.; Monterey, CA, October 21–25 2001; Kluwer Academic Publishers: 2001; pp 623–624.

GTG NH₂). The target for this study is 5'Cy5A₁₀. 5'NH₂ modified 41-mer oligo probes (CTC TGT TGT AAG TCA AGA ACG AGT GTG AGA GTG GAA AGT T), and its complementary oligomers were used for the limit of detection determination of the plastic microfluidic channel hybridization assays. During the assay, the target sample solution was pipetted into the hybridization channel and the access holes were sealed with tape. The device was put in the hybridization chamber at 50 °C for 60 min. The device was then removed from the hybridization chamber and washed with 1× SSC for 30 min before it was scanned on a GenePix 4000B array scanner (Axon instrument, Union City, CA).

Pluronics and Hydrophobic Membrane Valves. The integration of micro-PCR and biochannel hybridization was accomplished using Pluronics polymer phase change valves. Pluronics solution was prepared by dissolving Pluronics powder in cold 1× TBE buffer. The Pluronics valve was formed by preinjecting 30% (w/v) Pluronic liquid crystal gel into the valve structure at room temperature. Lowering the Pluronics gel temperature, below 5 °C, opened the pluronics valve. An air-permeable hydrophobic membrane (Durapore) was used to seal an access hole at the end of the hybridization channel. The membrane was acquired from Millipore (Bedford, MA).

RESULTS AND DISCUSSIONS

Device Fabrication. The CO₂ laser engraving system works like a printer. The fluidic network design is first generated with CorelDraw software on a computer, and then the laser cuts the work piece accordingly. A simple cross-channel structure fabricated in a black PC wafer of 250-μm thickness is shown in Figure 1b. A small portion of the channel is enlarged and shown in the upright corner of Figure 1b for a better view. The channel is 150 μm wide and the reservoirs, at the end of the channels, are 1 mm in diameter. The quality of the channel and circle structures is good, and no excess burning along the edges of the structure is observed. The minimum feature size achievable using this laser engraving system is limited by the spot size of the laser beam, which is ~150 μm in our system. Smaller feature size should be achievable by further focusing the laser beam. Because of the presence of carbon, which absorbs CO₂ laser energy more efficiently, black PC wafers have consistently yielded cleaner devices than transparent PC wafers of the same thickness. Therefore, thin black PC wafers were used to fabricate the middle pieces containing all the fluidic structures, and transparent PC wafers were used as covers to enclose the fluidic structures. The transparent PC cover also allows for optical detection after hybridization assays. Since no photomask is needed, this fabrication technique is extremely fast for building prototype devices. With the design being developed by using CAD software, devices with simple channel structures can be fabricated in just a few minutes.

Thermal bonding and adhesive tape bonding are the primary bonding techniques available in our laboratory for device assembly. However, neither one of these bonding techniques alone is sufficient for the fabrication of the integrated PCR hybridization devices. Double-sided adhesive tape bonding is fast and biocompatible with a hybridization reaction, but the adhesives on the tape are not biocompatible with a PCR. In addition, a PCR chamber formed by adhesive tape bonding cannot withhold the pressure generated during PCR thermal cycling. Thermal bonding produces

robust microfluidic structures, but the high temperature (139 °C), required for rapid PC bonding, damages the prespotted oligo probes in the hybridization channel. Therefore, the monolithic device was first thermally bonded without the hybridization channel enclosed. The hybridization channel was then enclosed with adhesive tape and reinforced with epoxy, after surface activation and probe attachment. The devices assembled this way did not leak under routine operation conditions. Selecting proper bonding technique and applying it to the proper structure assembly was key to the success of integrated device fabrication.

Pluronics Phase Change Valves. Microvalves are critical to the successful integration of PCR amplification with the DNA hybridization assay. Suitable microvalves have to meet a number of requirements. First, the valves have to be able to withhold the pressure generated during PCR, caused by degassing and air expansion at elevated temperature. If the valve fails, the PCR sample will be pushed out of the PCR chamber, resulting in a failed PCR. The amount of pressure required to prevent degassing was estimated by Chiou et al.²⁶ to be ~3.1 psi. The evaluation was performed using solubility data for air in water and Henry's law. The presence of an air gap between the PCR chamber and the valves will cause additional internal pressure buildup. This air gap will try to expand and generate additional 3.7 psi pressure at 94 °C (calculated using ideal gas law); therefore, the valve has to be able to withhold at least 6.8 psi total pressure to ensure the successful confinement of the PCR sample inside the PCR chamber during the PCR thermal cycling. Second, because valves will be in direct contact with PCR solution, the valve material should not inhibit PCR. Third, the valve should be opened easily after PCR and allow PCR solution to flow into the hybridization channel.

Pluronics F127, a commercially available surfactant, are uncharged (EO)₁₀₆(PO)₇₀(EO)₁₀₆ triblock copolymers. Solutions of Pluronics within a concentration range of 18–30% are low-viscosity liquids (<2 P) at low temperature (0–5 °C) but form self-supporting cubic liquid crystalline gels at room temperature.⁵⁰ Therefore, Pluronics solution at the proper concentration can be used as a one-shot, phase change valve. These one-shot valves are initially closed and become permanently opened once activated. We found that the presence of Pluronics molecules did not inhibit PCR. The concept of utilizing Pluronics liquid crystalline gel as one-shot phase change valves was then tested. The 30% Pluronics gel was introduced into four parallel fluidic channels, which connected to a circular chamber (Figure 2a). Green food dye was mixed with Pluronics gel to allow better visualization. The polycarbonate device was then placed on top of two 1-in. square Peltier TE cooler devices. The blue line in Figure 2 indicates the boundary between the two Peltier devices. Before the activation of the valves, the red testing fluid was stopped by the Pluronics valves, and the valve did not open at room temperature under 8 psi pressure (Figure 2a). When the bottom Peltier was turned on to cool the device to 5 °C, the 30% Pluronics gel in the bottom channel start to liquefy. The test solution was then pushed through the valve and into the circular chamber on the right under only 1 psi pressure (Figure 2b–d). Since the top Peltier remained at room temperature, the top three Pluronics

(50) Rill, R. L.; Liu, Y.; Van Winkle, D. H.; Locke, B. R. *J. Chromatogr., A* **1998**, 817, 287–295.

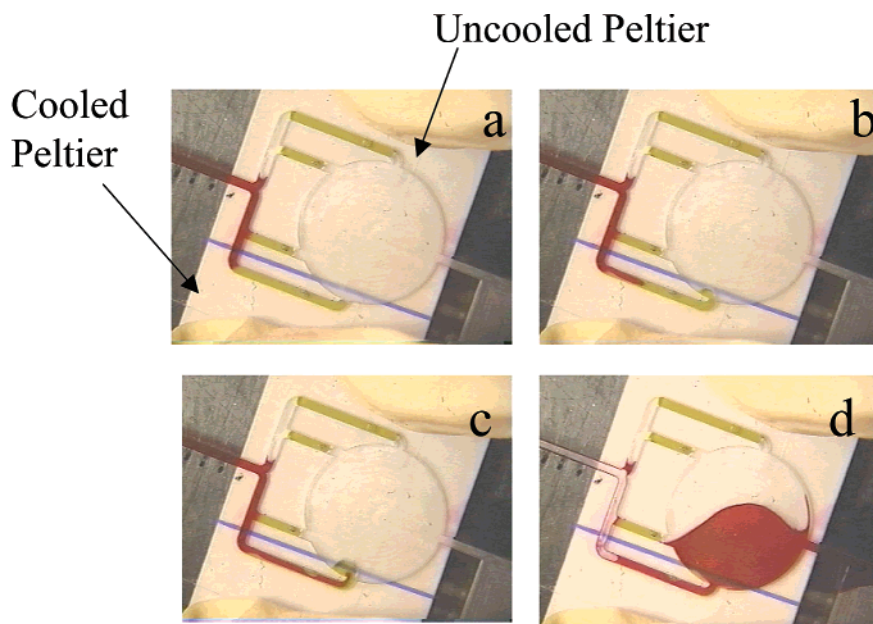


Figure 2. Demonstration of Pluronics polymer valves in fluidic channel structures. All the channels are 1 mm wide and 500 μm deep. The two shorter channels in the middle are 5 mm long, and the two longer channels at the outside are 10 mm long. Pluronics polymer valves were installed in these four channels, which connect the channel on the left and the chamber on the right. The device was placed on top of two Peltier devices (1 in. square) with their border in the middle indicated by the blue line. The top Peltier is always off. The bottom Peltier was off in (a) and was turned on to cool to 5 $^{\circ}\text{C}$ in (b–d).

valves remained closed. We found that a 30% Pluronics valve in a $9 \times 0.25 \times 0.25$ mm (the dimension of the valve structure) polycarbonate channel can hold 20 psi pressure, well above the 6.8 psi holding pressure required for PCR. The advantages of Pluronics temperature transition valves are their simplicity of implementation and operation. Although in solid gel form, Pluronics gel is not cross-linked and can be easily injected into the microfluidic valve structure to form a one-shot valve by using a preloaded syringe at room temperature. The Pluronics valves can be easily opened when valve temperature is lowered below the Pluronics gel transition temperature.

PCR Amplification. Planar serpentine PCR channel design was selected due to requirements of function integration and ease of fluid transfer. Polycarbonate has lower thermal conductivity than silica or glass, so the PC device was kept thin (wall thickness of 250 μm and chamber height of 250 μm) in order to achieve reasonable thermal cycle time. The temperature cycling performance of the device in a dual Peltier assembly is represented by three cycles of the program in Figure 3. The chamber temperature follows the Peltier surface temperature well, with very little time lag. The heating from room temperature (25 $^{\circ}\text{C}$) to denaturation temperature (94 $^{\circ}\text{C}$) takes ~ 9 s, corresponding to a heating rate of 7.9 $^{\circ}\text{C}/\text{s}$. The cooling rate is slower, ~ 4.6 $^{\circ}\text{C}/\text{s}$. Both heating and cooling rates compare reasonably well with those of conventional thermal cyclers (1–2 $^{\circ}\text{C}/\text{s}$). The time required for one complete cycle of denaturation, annealing, and extension is ~ 19 s, without counting the dwell time at each temperature. However, our home-built PCR thermal cycler, although effective, is not as user friendly as we would like. Improvement on the thermal cycler design is needed for easy realization of good thermal contact among device, thermal coupler, and Peltier surface.

The PCR amplification efficiency per cycle (Y) was estimated with symmetrical PCR amplification of *E. coli* 221-bp fragments

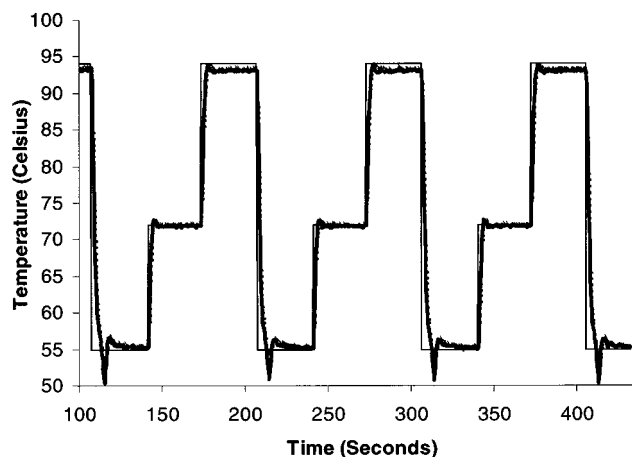


Figure 3. Thermal couple temperature readings of the PCR device and Peltier surface as a function of time during three cycles of PCR amplification: set temperature (thin solid line), top Peltier temperature (thick solid line), and device temperature (thin dashed line). The thermal cycle conditions are given in the Experimental Section.

using the following equation:

$$C_{\text{product}}/C_{\text{target}} = (1 + Y)^n$$

where C_{product} is the end concentration of product DNA, C_{target} is the initial concentration of template DNA, and n is the number of cycles.

The efficiency per cycle for micro-PCR device is 41% and compared well to the 47% efficiency of the commercial MJ PCR instrument. The reduced PCR efficiency could be due to the increased surface-to-volume ratio of our PCR devices.

This thermal cycler was used to perform A-PCR amplification of *E. faecalis* 195-bp fragments in the PCR portion of the device,

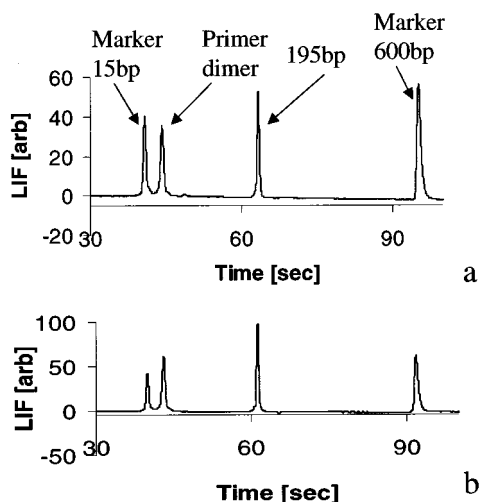


Figure 4. Off-chip electrophoretic analysis comparison of A-PCR amplifications of 195-bp fragments of *E. faecalis* genomic DNA performed in (a) a polycarbonate PCR device, on a PCR thermal cyclizer built in-house, (b) a 500- μ L polypropylene tube in MJ PCR thermal cyclizer. The Caliper LabChips were used as received and were run on an Agilent 2100 Bioanalyzer using a DNA 500 assay.

with Pluronic valves in place. Since single-stranded DNA was not detectable by conventional DNA dye staining methods, the double-stranded DNA produced in A-PCR was used to monitor the efficiency of the reaction. BSA (250 μ g/mL) was added to the PCR mixture to prevent adsorption of PCR polymerase or nucleic acids to the PC surface.⁵¹ Figure 4a shows the electropherogram of the *E. faecalis* 195-bp PCR product, amplified in the micro-PCR device and electrophoretically analyzed on the Agilent bioanalyzer. Amplification of the same PCR mixture was also performed using a commercial MJ PCR thermal cyclizer, and the analyzed result is shown in Figure 4b. The amount of dsDNA produced in the micro-PCR device is \sim 60% of that in MJ thermal cyclizer under the same reaction conditions. Additional experiments will be carried out in the future to further optimize reaction conditions and increase PCR efficiency.

Hybridization in Microfluidic Channels. One advantage, of being able to carry out DNA hybridization in microfluidic channels is that it facilitates the integration of a DNA hybridization assay with a sample preparation functional unit, in a lab-on-a-chip platform. To achieve a successful hybridization assay, it is important to have an efficient DNA probe attachment chemistry, a robust probe dispensing technique, an optimized hybridization protocol, and sensitive signal detection. Failure in any one of these aspects will result in poor assay quality or even in no signal at all. To evaluate the hybridization assay, Cy3-labeled oligo probes T₁₀ and probe D3488 were immobilized onto the PC surface of a microchamber, in a 2 \times 5 array, using Motorola proprietary DNA attachment chemistry. The target for this hybridization assay is Cy5-labeled oligo A₁₀ molecules. Therefore, D3488 probes serve as reference probes. The hybridization chamber has dimensions of 1.2 \times 5 \times 0.25 mm. After hybridization with Cy5-labeled oligo A₁₀ targets, the device was scanned at 532 nm. The fluorescent image of hybridization chambers is shown in Figure 5a. At 532-nm setting, only Cy3-labeled A₁₀ and D3488 probes were revealed,

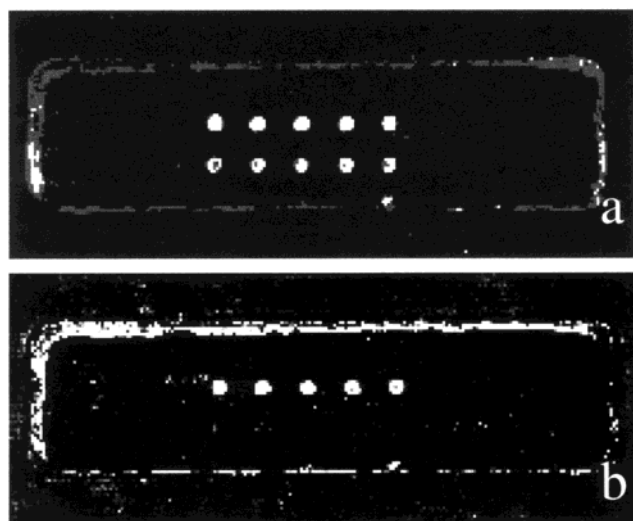


Figure 5. Evaluation of attachment and hybridization chemistry utilizing Cy3-labeled probes and Cy5-labeled targets. (a) Fluorescent image of hybridization chamber with laser scanning wavelength of 532 nm. The probes in the first row are 5'Cy3T₁₀, and the probes in the second row are probes 5'Cy3D3488. (b) Fluorescent image of hybridization with 5'Cy5A₁₀ targets. Laser scanning wavelength of 635 nm.

allowing evaluation of attachment chemistry and dispensing quality. Both probe sets were successfully dispensed and attached to the surface of the plastic fluidic chamber. The five spots in the first row of the 2 \times 5 array are oligo A₁₀, and the five spots in the second row are D3488 probes. The spot size is \sim 150 μ m with spacing between spots of 400 μ m. The shape of the spots is very well defined and shows good signal uniformity. Good spot quality reflects efficient attachment chemistry and a robust dispensing procedure. The device was then scanned at 635 nm, and the resulting fluorescent image is shown in Figure 5b. Cy3-labeled probes did not fluoresce with 635-nm excitation, and the observed fluorescent signal originates from the Cy5-labeled A₁₀ target molecules, which hybridized to the complementary T₁₀ probes. No fluorescent signal was observed in the second row of the D3488 probes; therefore, the fluorescent signal in Figure 5b is not due to nonspecific probe–target interaction. The background signal is low, and no nonspecific adsorption of target sample molecules was observed on the surface except at the edges of the well. We believe that the fluorescence of the well edges originates from target sample molecules trapped on the glue from the edge of the double-sided tapes used to construct the fluidic chamber device. This experiment provides evidence that the integrity of the device is good, allowing no sample solution to leak through the bonding interface. The limit of detection (LOD) of biochannel hybridization assay was evaluated using 5'NH₂-modified *S. sali* 41-mer oligo probes with their complementary oligomers as target. Good linearity was observed between the fluorescence hybridization signal and sample concentration for the target sample concentration range of 50 pM–10 nM, with an R^2 value of 0.985 (data not shown). No hybridization signal was detected at 10 pM concentration. The S/N ratio at 50 pM is 5.

Integrated Device for PCR and Hybridization Assay. **Design Considerations and Device Operation.** The integrated device is shown in Figure 6. The device contains a PCR chamber (38 μ L), a hybridization channel (7 μ L), a syringe coupled to a

(51) Witter, C. T.; Garling, D. J. *Biotechniques* **1991**, *10*, 76–83.

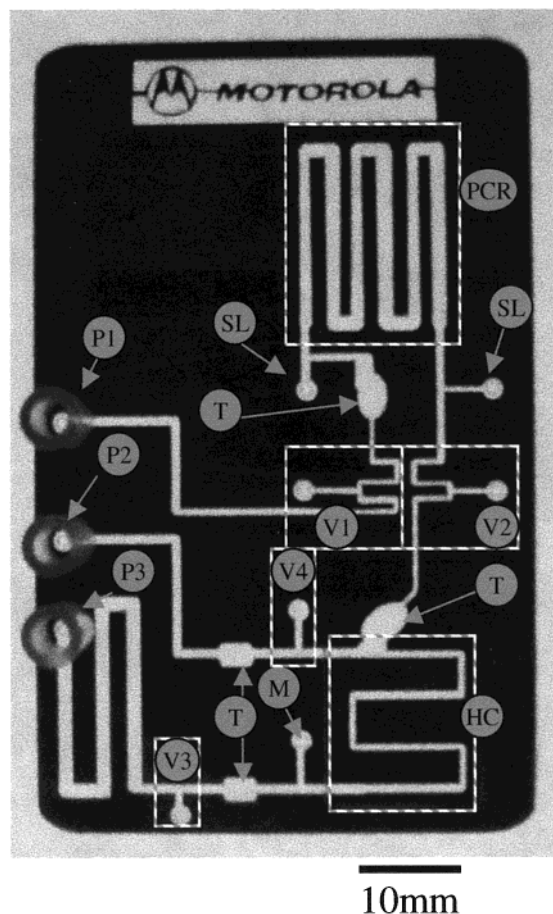


Figure 6. Monolithic integrated polycarbonate DNA assay device. Serpentine PCR channel (PCR), hybridization channel (HC), Pluronic valves (V1–V4), Pluronic traps (T), hydrophobic air-permeable membrane (M), PCR reagent loading holes (SL), sample driving syringe pump P1, waste-withdrawing syringe pump (P2), and wash syringe pump (P3).

hybridization wash solution channel (20 μL), a waste channel coupled to a waste syringe, four Pluronic trapping reservoirs, one hydrophobic membrane valve, four Pluronic valves, seven reagent introduction holes, and three external syringe pump interface reservoirs. The dimensions of the device are 5.4 cm \times 8.6 cm \times 0.75 mm and resemble that of a credit card. The PCR chamber volume (38 μL) is large relative to the current hybridization channel volume (7 μL). But this volume can be utilized in a longer hybridization channel with a higher density array. The hybridization channel was designed to accommodate efficient dispensing of probes, using the available SpotBot Personal Microarrayer. With this spacing, all four pins of the microarrayer were utilized, with no need for device position adjustment. It took the SpotBot \sim 10 min to dispense 120 probes into the four channels. Pluronic valves were installed before any reagent solution was introduced into the device. The two Pluronic valves adjacent to the PCR chamber enclose the PCR solution during the reaction. The first Pluronic valve (V1) isolates the PCR chamber from the external pump, and the second Pluronic valve (V2) is located between the PCR chamber and the hybridization channel. The third Pluronic valve (V3) is between the hybridization channel and the wash solution channel. The fourth Pluronic valve (V4) isolates the hybridization channel from the waste

chamber. PCR mixture and hybridization wash solution were introduced into their corresponding chambers on the device. Then all of the reagent access holes were sealed permanently by pressing down one layer of adhesive tape and one layer of Parafilm over the reagent holes.

During PCR thermal cycling, only the PCR chamber portion of the device was sandwiched between Peltier thermal electric heating units. After PCR thermal cycling, the two Pluronic valves adjacent to the PCR chamber were cooled to 5 $^{\circ}\text{C}$ with a Peltier thermal electrical device. Then the syringe pump (P1) was used to push the Pluronic valve solution and PCR amplification solution toward the DNA hybridization channel. When the Pluronic solution entered the Pluronic traps, located outside of the Peltier cooler zone, the Pluronic solution resolidified into a solid gel state and did not travel any further. This prevented the Pluronic gel from blocking the connecting channel to the hybridization chamber. The amplified PCR sample solution was then continuously pushed into the hybridization channel. The air-permeable hydrophobic membrane vent at the end of the hybridization channel allows air from the channel to flow out of the device, while sealing target solution that flows into the channel. Because of the small dimension of the fluidic channel, target DNA molecules are confined to the close vicinity of the capture probes. It was estimated that it only took \sim 30 min for a 200-base target to reach capture probes from the top of the channel by diffusion, assuming a target diffusion coefficient of $1.7 \times 10^{-7} \text{ cm}^2/\text{s}$.⁵² We determined experimentally that 1-h reaction time is sufficient for the detection of a hybridization event. Further improvement of hybridization efficiency could be realized when in-channel target solution oscillation was implemented in the future design. The Peltier device, underneath the hybridization chamber, was maintained at 50 $^{\circ}\text{C}$ during the 1-h hybridization reaction. After hybridization, the valves three (V3) and four (V4) were opened by the activation of syringe pumps P2 and P3. Since the pressure requirement is not as high as for V1 and V2, valves V3 and V4 were designed to hold less pressure and allow activation by syringe pumps alone. The first 10 μL of the wash solution was pushed into the hybridization channel, while the waste syringe withdrew the target solution. The next 10 μL of the wash solution was left in the hybridization channel to incubate for 20 min. The wash solution was manually removed by waste syringe before scanning. We attribute the successful integration of multiple functions on a monolithic device to the implementation of the pluronic valves. Of the 10 devices built and tested, Pluronic valves have worked each time. Only 2 of the 10 devices leaked because of thermal bonding failure during PCR thermal cycling. Plastic devices containing only fluidic channel structures are very inexpensive when produced in large quantity by injection molding. However, the cost of the device will go up if an additional complicated fabrication process is needed for implementing mechanical valves. The implementation of Pluronic phase change valves did not require additional device fabrication, and therefore, the devices with Pluronic valves could cost much less to build. Since the device is preloaded with all of the necessary reagents needed for the assay, potential contamination from human interference is eliminated, and automation is made possible.

(52) Jian, H.; Vologodskii, A.; Schlick, T. *J. Comput. Phys.* **1997**, *136*, 168–179.

DNA hybridization requires the presence of single-stranded DNA targets. To bypass a postamplification step for the denaturation of dsDNA, asymmetrical PCR was implemented into our assay. Asymmetrical PCR utilized strand biasing to preferentially amplify the target strand of choice. Three different types of probes were dispensed in four horizontal sections of the serpentine hybridization channel. The probe layout is identical in each of the four horizontal sections. There are two sets of 1×5 array of each type of probe in each horizontal channel section and a total of eight sets in the entire serpentine hybridization channel. Depending on which target DNA template molecules are present in the PCR chamber, the corresponding probes will light up after a hybridization event occurs. Figure 7 (1) is the fluorescent image of the hybridization chamber, using the *E. coli* 221-bp gene as amplification target. Hybridization reactions occurred at the sites of *E. coli* probes. Two sets of hybridization sites were enlarged for better view. The fluorescent signals of corresponding probes in the same array were very uniform. Interestingly, the fluorescent background inside the fluidic channel is lower than that from the surrounding ridges. One possible explanation is that thermal bonding causes increased roughness at the bonding interface and, therefore, causes an increase in scattered light during scanning. These integrated devices were also tested for *E. faecalis* gene^{195bp} amplification, detection, and multiplex PCR (*E. coli* and *E. faecalis*) amplification, detection. All amplification and hybridization reactions were successful, and the results are shown in Figure 7.^{2,3}

SUMMARY

We have successfully integrated PCR, hybridization, and hybridization wash functions into a single, low-cost, disposable monolithic device. The key to the success of the integrated device is the implementation of Pluronic phase change valves, which are capable of holding pressures greater than 20 psi, to meet on-chip microvalve requirements. An air-permeable hydrophobic membrane valve allowed for the movement of solution into otherwise airtight hybridization channel. The devices (750 μm in thickness) were fabricated using CO₂ laser machining and were assembled using a combination of thermal and adhesive tape bonding. The reagent transport on the device was provided by syringe pumps. The heating and cooling requirements were met by utilizing Peltier thermal electrical devices. Motorola proprietary oligo probe attachment chemistry was used for attaching probes in hybridization channel. Both single-target and multiplex A-PCR was performed on the *E. coli* gene and the *E. faecalis* gene and detected in these devices. One focus of future work will be the optimization of the PCR and the hybridization reactions, to achieve rare target detection. The second focus of future work will be

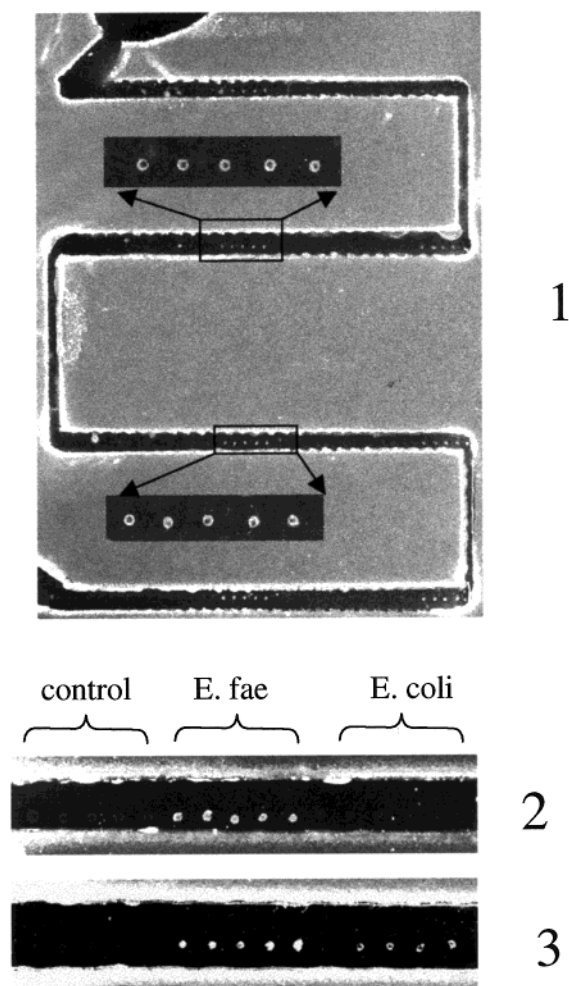


Figure 7. PCR hybridization results from monolithic integrated device. (1) *E. coli* 221-bp hybridization after amplification. Portions of the biochannel were enlarged for better viewing. (2) Fluorescent image of portion of biochannel after *E. faecalis* amplification and hybridization. (3) Fluorescent image of portion of biochannel after multiplex (*E. faecalis* and *E. coli*) amplification and hybridization.

introducing high-throughput assays in parallel multiple channels of an integrated device.

ACKNOWLEDGMENT

This research is sponsored in part by NIST under Contract 70NANB9H3012. The authors also thank Motorola Life Sciences for the use of their GenePix 4000B Array Scanner.

Received for review February 12, 2002. Accepted April 12, 2002.

AC020094Q